ment are more reliable than those from the TFEWR (and HREM), because the diffraction information extends about twice as far (0.14 nm for TFEWR versus 0.07 nm for electron diffraction) and because the diffraction information is not changed by the electron microscope aberrations. Therefore, we did not try to get the best fit between the experimental and the calculated exit waves. The R values obtained are very low compared with the R values of electron diffraction refinements reported in the literature (26). The lower R values result mainly from the inclusion of dynamic diffraction in our refinements, indicating the necessity for taking the dynamic diffraction into account. The structure of Mg_5Si_6 is very likely to be correct given the low R values obtained, the fit of the experimental and calculated exit waves, and the plausible interatomic distances and coordinations obtained for all atoms.

REFERENCES AND NOTES

1. A. Wilm, *Metall. Z. Ges. Höttenkunde* **8**, 225 (1911).
2. A. H. Geislet and J. K. Hill, *Acta Crystallogr.* **1**, 238 (1948).
3. G. A. Edwards, K. Stiller, G. L. Dunlop, *Appl. Surf. Sci.* **76/77**, 219 (1994).
4. G. A. Edwards, G. L. Dunlop, M. J. Couper, in *Proceedings of the International Conference on Aluminum Alloys*, Georgia Institute of Technology, Atlanta, GA, 11 to 16 September 1994 (Georgia Institute of Technology, Atlanta, 1994), p. 620.
5. S. J. Andersen, *Met. Mater. Sci.* **26A**, 1931 (1995).
6. D. Van Dyck and M. Op De Beeck, in *Proceedings of the 12th International Congress on Electron Microscopy*, International Federation of Electron Microscope Societies, Seattle, WA, 12 to 18 August 1990 (San Francisco Press, Seattle, WA, 1990), pp. 26–27.
7. W. Coene, G. Janssen, M. Op De Beeck, D. Van Dyck, *Phys. Rev. Lett.* **69**, 3743 (1992).
8. J. Jansen, D. Tang, H. W. Zandbergen, H. Schenk, in preparation. MSLS uses a standard algorithm to minimize the R value. To determine the gradient of the R value as a function of the thickness, we added a very thin slice at the exit plane of the multislice calculation. To determine the accuracy of MSLS, we applied it on several compounds with known structures (LaNiBN, $La_3Ni_2B_2N_3$, $Ce_5Cu_{19}P_{12}$, $Ba_2Ca_3Cu_5O_{10}$, and $Ba_2Ca_2Cu_4O_8$) determined by x-ray single-crystal diffraction or neutron powder diffraction. The MSLS refinement resulted in very similar (a difference in atom positions less than 0.01 nm and on average less than 0.003 nm) atom positions. Putting one or more atoms at the wrong position gives much higher R values.
9. The material investigated was Al with 0.2 weight % Fe, 0.5 weight % Mg, 0.53 weight % Si, and 0.01 weight % Mn, extruded as described in (5) and aged at 185°C for 5 hours.
10. The information limit is not circular but elliptical (0.135 nm by 0.150 nm), because of the anisotropic response of the microscope to external vibrations.
11. Other reasons to cool the specimen are the reduction of the electron beam induced contamination and amorphization. Unfortunately, commercial sample cooling holders do not allow real HREM imaging; thus it is difficult to do electron diffraction and HREM on the same precipitates.
12. I_{obs} and I_{calc} are the intensities of the reflections. The significant reflections are $I_{obs} > 2\sigma(I_{obs})$, where $\sigma(I_{obs})$ is the standard deviation of the reflection.
13. EDX element analysis was done with a Link EDX element analysis system, and the mineral forterite was used to calibrate the Cliff-Lorimer factor for these two elements.
14. K. Matsuda, S. Tada, S. Ikeno, T. Sato, A. Kamio, *Scr. Mater.* **32**, 1175 (1995).
15. S. Andersen *et al.*, in preparation.
16. W. Coene, A. Thust, M. Op De Beeck, D. Van Dyck, *Ultramicroscopy* **64**, 107 (1996).
17. The frequency-dependent delocalization or information shift, S, of the shape has been described in (27) and is $S = \varepsilon \lambda \mathbf{g} + C_s \lambda^3 \mathbf{g}^3$, where ε is the defocus, λ is the wavelength, C_s is the spherical aberration, and $\mathbf{g}$ is a reciprocal lattice vector. For instance, for a 300-keV microscope with a point-to-point resolution of 0.2 nm (C_s = 1.2 mm) at Scherzer focus (optimal focus) (−60 nm), S of the 0.1-nm frequency ($\mathbf{g}$ = 10 nm⁻¹) is 8.4 nm, and S is 0.6 nm and −0.04 nm for the 0.2-nm frequency ($\mathbf{g}$ = 5 nm⁻¹) and 0.3 nm ($\mathbf{g}$ = 3.33 nm⁻¹) frequency, respectively.
18. For the TFEWR, series of 20 HREM images were recorded with focus increments of 5.2 nm. The starting focus was about −70 nm. The images were recorded with a 1024 by 1024 pixel slow scan charge-coupled device camera.
19. Further analysis of this exit wave, such as the atomic structure at the interface between β″ and the Al matrix and the structure and the origin of the defect in the β″ precipitate, is given elsewhere (15).
20. Because of the overlap with the Al reflections, the 10% discarded reflections are rather random for the structure of the precipitate, which implies that the accuracy of the structure determination is not substantially hampered by this omission.
21. The space group could have been determined by convergent beam electron diffraction, but given the small size of the precipitates, this method was not used.
22. To approximate a kinematic refinement with the MSLS program, a very small thickness (for example, 1 nm) or a very low occupancy should be used. The latter approach was used because in this way the excitation error of the diffraction spots is properly taken into account. This excitation error occurs because, in contrast with x-ray single-crystal diffraction in which each diffracted beam is measured at its maximum (reflections are in exact Bragg condition), most diffracted beams in electron diffraction are not in exact Bragg condition. In the calculation of the kinematic R values, a 1% occupancy of all atom sites and the thicknesses obtained for the dynamic refinement were used.
23. It would be better to do a complete refinement with the addition of an Al matrix in front and after the precipitate and to refine the thicknesses of these two layers as well. This, however, is not yet possible with the MSLS package.
24. For the simulated exit wave, the following parameters were used: defocus spread, 10 nm, which is used to impose an information limit of about 0.14 nm; specimen thickness, 10 nm; convergence angle, 0.1 mrad; and crystal tilt, 1.5° about the [20$\bar{1}$] direction. The specimen tilt and thickness were roughly estimated from the loss of symmetry in the surrounding Al matrix. The agreement between the calculated and the experimental exit wave can be improved by adjustment of the twofold astigmatism and beam tilt, but this would be merely a cosmetic improvement without giving any proof of the reliability of the model.
25. The orientation relation is $[100]_{\beta''}//[230]_{Al}$, $[010]_{\beta''}//[001]_{Al}$, and $[001]_{\beta''}//[310]_{Al}$.
26. D. L. Dorset, *Structural Electron Crystallography* (Plenum, New York, 1995).
27. W. Coene and A. J. E. M. Jansen, *Scanning Microsc. Suppl.* **6**, 379 (1992); H. W. Zandbergen, D. Tang, D. Van Dyck, *Ultramicroscopy* **64**, 185 (1996).
28. The Al-Mg-Si specimen was supplied by HYDRO Aluminum AS (Sunndalsøra, Norway). Stichting Technische Wetenschappen is acknowledged for financial support. We thank D. van Dyck and M. op de Beeck for discussions. S.J.A. is indebted to Norsk Hydro Al for financial support.

Competing Interactions and Levels of Ordering in Self-Organizing Polymeric Materials

M. Muthukumar, C. K. Ober, E. L. Thomas

The sophisticated use of self-organizing materials, which include liquid crystals, block copolymers, hydrogen- and π-bonded complexes, and many natural polymers, may hold the key to developing new structures and devices in many advanced technology industries. Synthetic materials are usually designed with only one structure-forming process in mind. However, combination of both complementary and antagonistic interactions in macromolecular systems can create order in materials over many length scales. Here polymer materials that make use of competing molecular interactions are summarized, and the prospects for the further development of such materials through both synthetic and processing pathways are highlighted.

Structural order over many length scales can be created in self-organizing materials by the presence of several molecular interactions including (i) hydrophobic and hy-

M. Muthukumar is in the Department of Polymer Science and Engineering, University of Massachusetts, Amherst, MA 01003–4530, USA. C. K. Ober is in the Department of Materials Science and Engineering, Cornell University, Ithaca, NY 14853–1501, USA. E. L. Thomas is in the Department of Materials Science and Engineering, Massachusetts Institute of Technology, Cambridge, MA 02139–4307, USA.

drophilic effects, (ii) hydrogen bonding, (iii) coulombic interactions, and (iv) van der Waals forces (1). The idea of combining interactions in the design of new synthetic macromolecular materials is just starting to be explored systematically. Within this framework, polymer scientists are currently attempting to bridge the extremes of the precision and elegant complexity of many biological materials and the statistical nature and relative simplicity of most synthet-

ic polymers. Polymer technology can benefit from new materials with controlled internal dimensions ranging from nanometer to macroscopic scales. For example, the design of photoresists with feature sizes now approaching the dimensions of only a few polymer chains will permit exploitation of such materials for higher density chips. Precise positioning of each molecular component needed for imaging and etch resistance in the thin photoresist layer is critical to this advanced technology (2). In this circumstance, controlled microphase separation and surface segregation may prove to be useful tools. It is also of technological importance to create structures with dimensions comparable to the wavelength of light wherein many opportunities exist, for example, in various optoelectronic applications (such as waveguides, photonic bandgap materials, and organic light-emitting diodes). In this article, we review the conceptual issues encountered in this undertaking, progress that has been made to date, and future directions.

Chemical function as well as physical function is induced in biological materials by the creation of specific shapes or conformations in the macromolecular structure, and the essential features of self-assembly in biological processes are well recognized. For example, to act as enzymes, proteins require specific chemical sequences, but these elements must fold up into a required shape to create a substrate-specific docking site, and the protein itself must avoid aggregation to stay in solution or incorporate itself into a membrane layer. Combinations of several interactions create minima in the local free energy as a function of different chain conformations for proteins. Without these types of interactions, entropy causes synthetic polymers with their much less complex sequences to adopt irregular shapes with little organization. However, such ordering influences, if present, can produce shapes and structures in a particular macromolecule and organize an assembly of such molecules into even larger structures with distinctive morphologies and properties.

Theoretical Basis of Self-Organization

The basic principles of the spontaneous organization of melts and solutions of simple synthetic polymers are well understood from both theory and experimental studies (3). Self-organization occurs from nanoscopic to macroscopic length scales and includes, for example, phase separation, microphase separation (4), mesophase formation (5), adsorption, and crystallization.

Just as for the peptide chains, a full understanding of the formation of ordered polymer structures requires a knowledge of the free energy landscape associated with different possible configurations of polymer molecules. The calculation and measurement of energy (E) and entropy (S) at the molecular level are nontrivial tasks; therefore, it is necessary to develop certain guidelines so as to successfully fabricate structures at different length scales.

Polymer molecules, because of the way their building blocks are covalently tethered together, can change from one configuration to another only in certain ways. This results in separate and distinct paths in the free energy landscape connecting the various configurations of a given polymer. The values of the free energy barriers existing between these configurations are dictated by the details of competing interactions among various building blocks and the entropy associated with particular ways of assembling topologically connected objects such as polymers. Although the above argument is for assembling one polymer molecule, subtle differences in free energy (F) and definite kinetic pathways between different structures also emerge during the self-organization of materials consisting of many polymer molecules. In the latter case, the scales of length and time are much larger.

There are basically three guiding principles that offer strategies to explore different length scales in self-organizing structures (biological or synthetic).

The first principle is of competing interactions and sequences. As a hypothetical example, consider an assembly of a multidomain polymer (MDP) with four domains strung together linearly. Such materials exist in the biological world, for instance, viral protein coats, enzymes, and other large macromolecular assemblies, but they are as yet unknown in the synthetic world. Each domain has the desired chemical functionality in terms of, for example, the number of hydrogen-bonding groups. The potential nature of each domain can be represented by strength q and a sign ($+$ or $-$). One domain q_1+ and another q_2- are complementary to each other and, if adjacent, will stabilize the structure by an energy q_1q_2. Domains of the same sign destabilize the structure by an energy q_1q_2 when they are neighbors. Now consider only two sequences, a and b, shown in Fig. 1A, connecting four domains with potentials $q+$, $1-$, $1+$, and $q-$. Sequences a and b are among six possible sequences where the domains occupy the corners of a regular square (Fig. 1). Note that in the "blocky" sequence a, the domains with the same sign are separated by the side of the square while for sequence b,
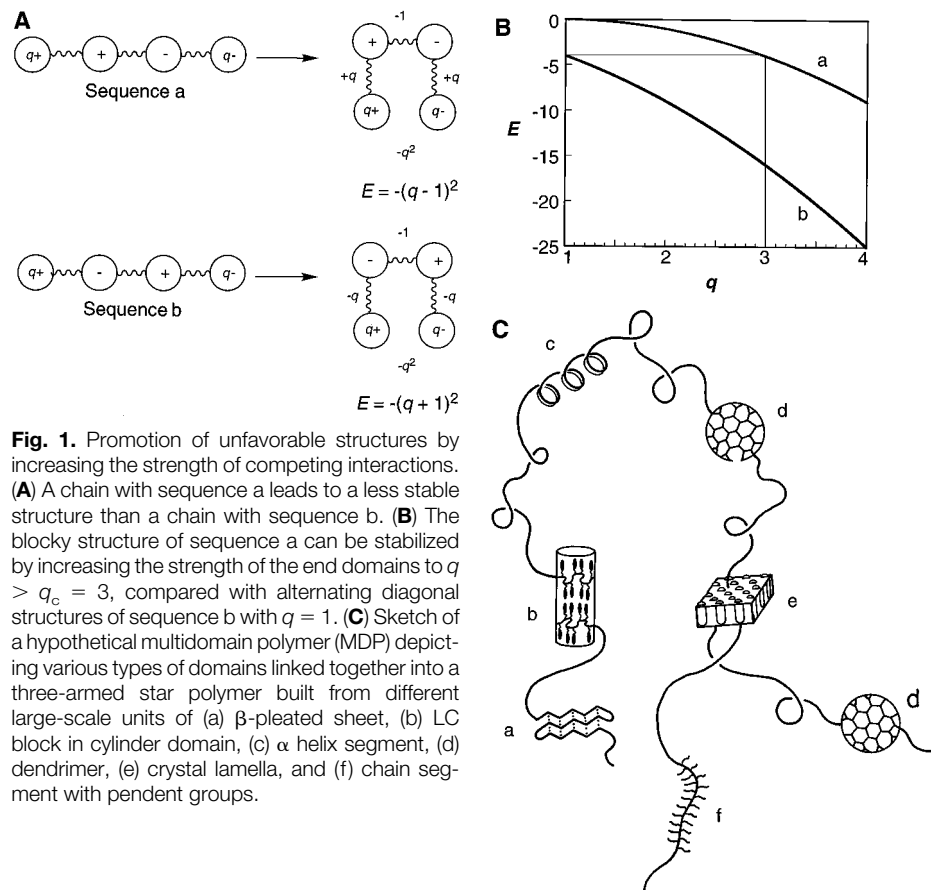
Fig. 1. Promotion of unfavorable structures by increasing the strength of competing interactions. (**A**) A chain with sequence a leads to a less stable structure than a chain with sequence b. (**B**) The blocky structure of sequence a can be stabilized by increasing the strength of the end domains to $q > q_c = 3$, compared with alternating diagonal structures of sequence b with $q = 1$. (**C**) Sketch of a hypothetical multidomain polymer (MDP) depicting various types of domains linked together into a three-armed star polymer built from different large-scale units of (a) β-pleated sheet, (b) LC block in cylinder domain, (c) α helix segment, (d) dendrimer, (e) crystal lamella, and (f) chain segment with pendent groups.

For panel A, sequence a: $E = -(q - 1)^2$

For panel A, sequence b: $E = -(q + 1)^2$

the same signed domains are separated by the diagonal. The interaction energies for sequences a and b are $(q - 1)^2$ and $(q + 1)^2$, respectively, accounting for only the nearest neighbor interaction.

Sequence b always leads to more stable structures for any value of q with similarly signed domains diagonally oriented (ignoring the entropy of a flexible spacer group denoted by the wiggly lines) (Fig. 1B). But if we want to create a structure with blocky (edge) orientation using sequence a that is more stable than the structure of $+ - + -$ (that is, sequence b with $q = 1$), then Fig. 1B requires that we increase the interaction strength of the end domains to a value of q greater than $q_c = 3$ (where q_c is the strength at the critical value). Thus, we can stabilize unfavorable structures by careful promotion of competing interactions among domains of a MDP with underlying desired sequences. This example also emphasizes the importance of sequence in stringing domains together. An example of a hypothetical complex MDP is sketched in Fig. 1C, where various functional building blocks (domains) are connected through covalent bonding with the use of flexible spacer segments. In this case, the domains replace monomers as building units in polymer synthesis.

Typically, biological polymers such as proteins do not have long blocky sequences but synthetic polymers do, and this provides an opportunity to manipulate organization if the assembly processes are well understood. An example that combines features of both the synthetic and biological world is the work of Tirrell and co-workers, who have created precisely tailored proteins with blocky structures (6). In these materials, blockiness was exploited to produce folded crystals with fluorinated groups on the crystal surface.

The second principle is of entropic frustration and topological dereliction. The entropy associated with different ways of cooperatively arranging various domains leads to a rugged and hilly free energy landscape, so this needs to be modified to guide the evolution of the emerging structure to obtain the desired overall pattern. In particular, the often blocky nature of synthetic polymers leads to strong influences by these factors. The devastating role played by the multiple pathways arising from the entropy of polymers and guidelines for the avoidance or use of this occurrence are illustrated by the following exactly solvable model (7). For specificity, consider the self-association of four domains sequentially connected by spacer links, each with $m - 1$ segments. There are four distinct ways any two of these domains can pair (Fig. 2A, configura-

tions a to d); let $-\varepsilon$ be the energy when two domains pair by approaching each other within a certain distance, and let the entropy associated with this pairing be $-ms/MT$. M is the total number of segments between these two domains and $-s/T$ is the entropy associated with making a loop of length m (where s is the temperature-dependent entropic contribution and T is temperature). The free energies of the topological states are $-\varepsilon + s$, $-\varepsilon + s/2$, $-\varepsilon + s/3$, and $-\varepsilon + s$ for the four configurations, respectively.

Although the most stable state with only one pair is that of configuration c in Fig. 2, its further evolution is to a two-pair state (Fig. 2, configuration g) with higher free energy ($F = -2\varepsilon + 9s$) and not to the lowest free energy state (Fig. 2, configuration e, with $F = -2\varepsilon + 6s$). The configurations e and g in Fig. 2 cannot be directly interconverted. The only way the state of g can be relaxed to that of e is if the trajectory is retraced backward to its original state and another attempt is made to avoid the intermediate metastable state. This effect is generic and seriously magnified when many more pairings need to be made instead of just two.

The above argument illustrates the inevitability in polymers of "topological dereliction" due to the local minimization of F. There are three ways to help proceed to the desired structure. First is to considerably reduce the number of possible topological states for a given number of pairings between domains by making the sequence tighter through reduction of the spacer length. This effect drastically reduces the number of different pathways. Second is to tune the value of the pairing energy ε to small values (by using weaker interactions) so that the energy pathway is smooth. Third is to provide an external field to the evolving system at opportune times to guide the system to reach the desired final (not necessarily equilibrium) structures at the expense of more complex processing conditions. The nature of the external field depends on the system; examples are chaperons for biological molecules, patterned surfaces for artificial catalysis and sensors, chemical potential gradients through solvent evaporation for self-assembly of block copolymers, magnetic or electric fields or both for annihilation of defects in liquid crystalline (LC) systems, and flow fields for orientational control in block copolymers.

The third guiding principle is the spontaneous selection of primary length scales. Many polymeric liquids self-assemble spontaneously into ordered structures with well-defined symmetry and dominant characteristic lengths. The mechanism of selection of a primary length scale is generic, but consider the case of diblock copolymers as a

specific example (two sequences of distinct monomers X and Y covalently linked together, . . .XXXX-YYY. . .). After primary length scales are selected in the system, the density of any component is nonuniform in space. Defining the local density of one of the components, say X, with respect to that in the homogeneous, disordered state as the order parameter $\psi(r)$ (where r is the spatial location), there are well-established statistical mechanical procedures to derive F of the system in terms of $\psi(r)$, after coarse-graining local details of the system (8):

$$F = (1/2)\Sigma_k\Gamma(k)\,\psi_k\psi_{-k} \qquad (1)$$

where $\psi(r)$ is decomposed into the Fourier modes (k being the reciprocal wave vector), and $\Gamma(k)$ is of the form

$$\Gamma(k) = A + Bk^2 + C/k^\alpha \qquad (2)$$

where A, B, and C relate, respectively, to chemical mismatch, interfacial tension between X and Y, and long-range correlations, and can be determined from scattering measurements as a function of temperature. The value of k (say k^*) that minimizes F determines the inverse of the primary length scale for a given system. It follows from Eq. 2 that

$$k^* = (\alpha C/2B)^{[1/(\alpha+2)]} \qquad (3)$$

Thus, we can tune the scale of spontaneously selected primary characteristic length by changing the interfacial tension (B) and the nature of long-range correla-
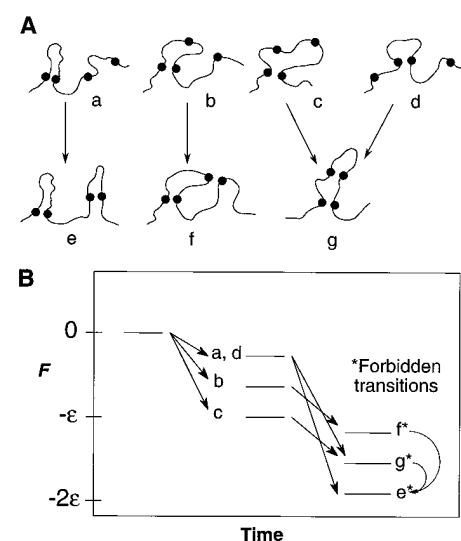
Fig. 2. Topological dereliction due to metastability. (**A**) Possible topological states for the model considered are configurations a to g, and their free energies with allowed pathways are sketched in (**B**). Spontaneous attempt to achieve the most favored state c in the immediate future leads to an unfavorable state g at later times. The direct conversion of g to the more stable state e is forbidden without returning to the starting point.

tion (C and the exponent α). The importance of the above argument is that if $\Gamma(k)$ of a system can be of the form given in Eq. 2, then that system self-organizes with spontaneous selection of a length scale comparable to $1/k^*$, independent of the molecular origins of the various terms.

Methods of Self-Organization in Synthetic Materials

Strategic design for materials with multiple length scales. In designing such materials it is essential to identify a pathway for obtaining a well-defined final structural state with order on multiple length scales starting from an initial homogeneous mixture of components. Expressed in terms of free energy, the evolution of the structure requires an overall reduction in the system entropy with a concomitant strengthening of intra- and intermolecular interactions. The design strategy for the formation of complex ordered structures is to organize from the largest length scale to the smallest, inducing a global pattern, followed by the sequential development of finer details (9).

If we wish to take advantage of anisotropic structures that can display a greater range of physical and chemical properties and functions than a homogeneous, isotropic material, then we must understand and control symmetry from the global to the local level. Thus, the selection of a particular growth direction with an applied bias field (such as flow, electric, or magnetic fields or the substrate surface) can produce highly textured or even "single-crystal" hierarchical structures. Then, within the material, a series of competitions determines the spontaneous selection of a set of primary length scales, topological relations, and structural symmetries.

Often the competitions needed to induce a specific structure are phase transitions such as helix-coil or crystallization, and the primary length scale for a particular competition is determined from the minimization of the relevant F. An example of a biological material where such effects are believed to occur is spider silk. Large, soluble protein units are coulombically assembled from an isotropic solution immediately before spinning to induce an oriented lyotropic solution. The LC silk solution passes through a long narrow duct, which applies flow orientation, and the assembled units organize to form both crystalline and amorphous regions and yield a water-insoluble, high-modulus fiber of extraordinary toughness (10).

In each subsequent free energy competition, the prior structures impose certain boundary constraints to maintain overall respect for the initial global symmetry. If the prior structures impose certain boundary constraints and the developing symmetry is different from the parent symmetry, defects must occur. Moreover, if the prior symmetry is strongly enforced on the new finer level of structure, such defects may be periodic. As a system organizes at ever smaller dimensions, the pattern selection is increasingly determined by the need for commensuration of the emergent length scales with existing ones and compatibility of structure across interfaces (for example, anchoring conditions). Therefore, control of very large length-scale molecular structure (of the order of the wavelength of light) in both biological and synthetic macromolecules requires avoiding the independent (and therefore uncorrelated) nucleation and growth of the ordering regions because their subsequent mutual impingement gives rise to a myriad of defects with spacings typically on the order of a micrometer (such as grain boundaries, dislocation, and disclination line defects). Such defects in the system may only slowly annihilate to reach a final thermodynamic equilibrium. The kinetics of this process is equivalent to the situation of topological frustration, except that scales of length and time are much larger.

Although the foregoing scenario is general and admits to an infinite set of possible components and an unlimited range of process variables, specific synthetic lines of approach toward the goal of sophisticated self-organized materials are appearing, as will be described below. The large synthetic units for a molecular structure (as in the case of spider silk) may be preassembled units of high molar mass with targeted intramolecular shapes and interaction sites for preferred packing. Placement of specific chemical groups for chirality, intermolecular docking, and so forth is done during synthesis with the intention of influencing tertiary and higher ordered structures. Successful synthetic designs will need to pay more attention to specific process pathways for structural organization and thus better integrate the synthesis and processing.

Use of molecular interactions. Synergistic interactions are a key element in attaining a desired overall structure and can be simultaneous (whereby several interactions bias toward the same structure) or sequential (whereby the first interaction in play sets up constraints at one length scale favorable to the subsequent interactions that develop order at other length scales). Currently, chemical synthesis does not design for materials that best bring about a series of structural transition steps leading to the final desired ordered material. Rather, a number of synthetic self-organizing materials have been created that depend essentially on a single molecular interaction. The importance of these materials is significant because they provide the basis for future materials that will require multiple organizing processes. A brief summary of such synthetic materials is given below in the context of the types of molecular interactions mentioned previously, followed by examples of materials in which several organizing processes have been combined in a single material.

A hydrogen bond is a highly directional, intermediate-strength, reversible interaction. As an example of how to construct interesting materials using a single type of interaction, Lehn and co-workers have introduced into oligomeric units base-pair structures that imitate nucleic acids. By preparing matched base-pair segments, his group produced molecular ropes that intertwine to form strands of complexed units that mimic some of the natural fiber-forming polymers but are held together entirely by hydrogen bonds (11). Similar base-pair chemical groups have been introduced by Stadler *et al.* (12) into elastomers to form thermally reversible networks by taking advantage of the modest thermal stability of these weak noncovalent bonds.

Fréchet, Kato, and co-workers (13) and others (14) have used single hydrogen bonds, which lack the specificity of the matched base-pair approach, to successfully attach LC groups to hydrogen-bonding polymer backbones. These structures are thermally stable at the required processing temperatures and enable a "molecular Lego" approach to macromolecular design, because one particular backbone can be easily modified with a variety of hydrogen-bonding groups. In other cases, simple surfactants have been hydrogen-bonded to polymer backbones to create ordered mesomorphic materials (15) and in some cases render otherwise insoluble, conjugated polymers both electrically conductive and processable in a self-ordered form (16).

Along with hydrogen-bonding, π-stacking interactions between aromatic rings have been used by Stoddard and co-workers (17) to construct catenanes, large interlinked molecular ring structures with oligomeric properties. Such materials display unusual optical properties and suggest ways in which self-ordering before chemical assembly may be carried out in larger systems. An example of this is the preparation of rotaxanes, macromolecules in which a polymer backbone is threaded through several macrocycles and locked in place by capping the chain ends (18). Practical applications in biochemistry are developing as the synthetic protocols are being created.

Another strategy involves the formation of complexes between polyelectrolyte mol-

ecules and oppositely charged surfactant micelles. Typically, many surfactant micelles adsorb on a single polyelectrolyte chain. The stability and size of such complexes can be adjusted by the ionic strength of the solution and charge density of the micelle. Complexes between polycations and proteins of net positive charge can be produced by using negatively charged patches on the protein surface. Other research has focused on building solid-state materials by combining polyelectrolytes and surfactants (*19*). In this circumstance, the shape contour of the surfactant molecule (for example, a single or double aliphatic chain) is extremely important in the condensed phase and will establish the type of mesomorphic order retained in the complex.

The question of molecular shape is of primary importance for the design of liquid crystals and LC polymers. Recent work by Percec has shown that wedge-shaped molecular units, when polymerized, can stack in the form of regular arrays of cylinders, as shown by both x-ray diffraction and transmission electron microscopy (*20*). On the nanometer scale, these latter materials combine LC behavior with a molecular-level mesoscopic recognition and provide hints for building MDPs, which can combine to form larger scale self-organizing elements.

Spontaneous selection of length scales. Although local, directed interactions are useful in forming complex polymer structures, larger structures can form through nondirectional weak interactions (such as van der Waals interactions, leading to macrophase

and microphase separation). When an initially homogeneous two-component polymer blend undergoes phase separation, composition fluctuations with characteristic lengths above a certain critical value [dictated by quench depth (undercooling below the equilibrium transition temperature) and interfacial tension] grow in size and decrease in number with time. Eventually the system ripens, with the longest wavelengths of macroscopic dimensions dominating, and two phases coexist. For polymeric systems this phase separation process can be nonuniversal. For example, when blends with sufficiently off-critical composition are quenched to a temperature well below the coexistence curve, phase separation often does not proceed to completion. Instead, domains with a relatively narrow distribution of sizes form because the transport of polymer chains across the interfaces differs for the two polymers. The sizes of the domains in such strictly nonequilibrium but extremely long-lived structures can be adjusted by modification of the quench depth and the degree to which the mixture's composition is off-criticality (sufficiently far away from a critical value on a phase diagram) (*21*). The metastable structures can be permanently pinned by further chemical reaction among the components, triggered, for example, by cross-linking with ultraviolet radiation.

In block copolymers with well-controlled architectures, microphase separation produces equilibrium periodic structures that can be selected by chemical design

(*22*). The selection of a primary length scale in coil-coil diblock copolymers was discussed above. By adjusting the degree of chemical incompatibility χ between the two blocks, the degree of polymerization *N* of the polymer, and the composition (*f* being the fraction of X monomers in each diblock copolymer chain), length scales associated with self-assembled structures are typically in the 10- to 100-nm range. The symmetry of the equilibrium morphology and the degree of segregation depend on χ, *N*, and *f*. For A-B diblocks in the strong-segregation regime, as the volume fraction of A increases, the periodic structures are alternating lamellae of A and B, hexagonally packed cylinders of B in a matrix of A, and BCC-packed spheres in a matrix of A. Inverse morphologies occur as the volume fraction of the B block increases. At lower degrees of segregation, in a narrow composition window between the hexagonal and lamellar phases, bicontinuous morphologies have been reported—double-gyroid, hexagonally perforated layers, and hexagonally modulated layers—some of which are only metastable. These periodic structures are quite similar to, but occur at larger size scales than, the many phases found in binary and ternary blends of natural and synthetic surfactants and oil and water (*23*).

Balancing Organizing Forces

If one or more of the components of a diblock copolymer itself has an inherent capacity to order in some way, then we can

Fig. 3. Examples of the occurrence of novel smectic phases in rod-coil diblocks due to the evolution of self-assembly through three successive phase transitions, resulting in global ordering over the 1-nm to 200-nm to 1-μm scale. (**A**) Alternating PHIC and PS layers arranged in a zigzag fashion. The PS domains appear dark because of preferential staining by RuO$_4$. Because the rod block is much longer than the coil block, the rods tilt with respect to the layer normal and interdigitate forming a S$_C$ structure [from (*27*)]. $\hat{n}$ = PHIC chain axis direction, $\hat{p}$ = lamellar normal, and *a* = angle between $\hat{n}$ and $\hat{p}$. (**B**) Another novel morphology called the "arrowhead" phase corresponding to a S$_O$ structure occurs when the volume fraction of the rod component is very high (98%) [from (*27*)]. Alternate domain boundaries comprise discrete PS regions that point in opposite directions. (**C** and **D**) The nature of the phase-separated microstructure is important in determining the arrangement of the LC groups pendent to the polymer chain in side group block copolymers. Here, the preferred parallel alignment of the mesogens with respect to the interface can be seen in (C), a lamellar phase, and (D), a LC cylinder phase [adapted from (*28*)].
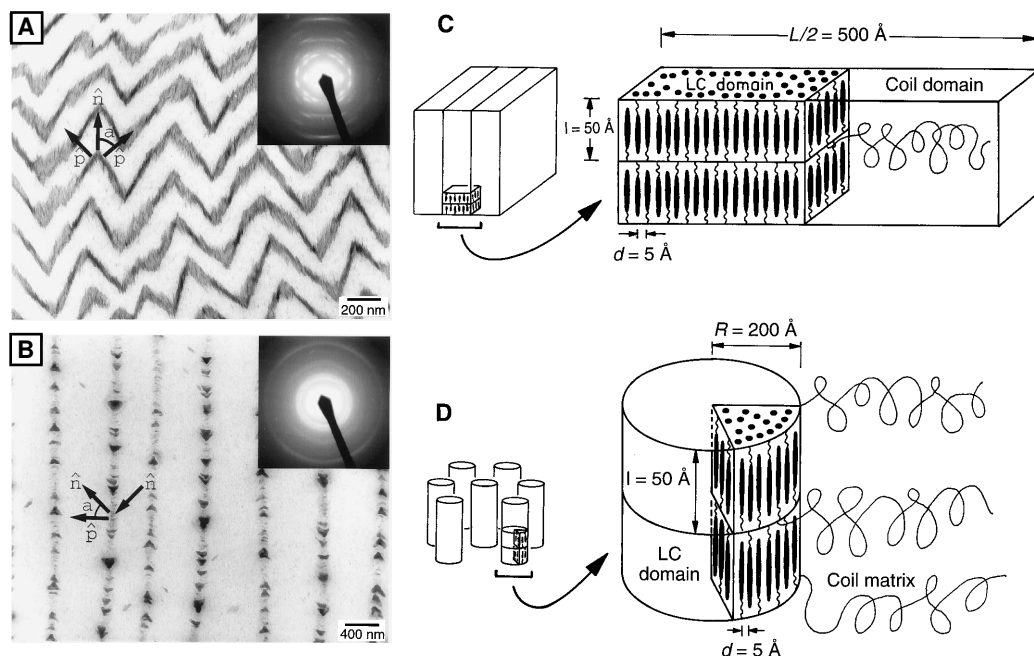
Fig. 4. (**A**) Schematic of the solid-state structure of a semifluorinated lamellar block copolymer. The interplay of phase separation and liquid crystallinity leads to alignment of the fluorinated mesogenic groups (indicated by green elongated rods), which are packed in smectic layers and lie parallel to the plane of the lamellae. The black segments in the blue background represent the coil block lamellae. At the upper surface region, the mesogenic groups are instead directed normal to the air, leading to remarkably stable, low-energy surfaces. The importance of surface and interface interactions is highlighted in these materials. (**B**) XPS results of intensity versus energy at two take-off angles with appropriate signal analysis show that the surface region of the block copolymers is almost exclusively the fluorinated block. Open circles, profiling depth = 4.5 nm at a take-off angle of 35°; filled circles, profiling depth = 8.1 nm at a take-off angle of 90°. (**C**) Schematic of the chemical structure of the semifluorinated block copolymer showing the structure of the semifluorinated side groups studied. (**D**) Small-angle and wide-angle x-ray diffraction measurements demonstrating that the smectic semifluorinated groups align parallel to the lamellar layers in the bulk. The meridional 00l reflections for the lamellar spacings can be readily observed as can the equatorial reflections for the smectic layer spacings for the semifluorinated groups. This sample spontaneously adopted this arrangement during the solvent casting process.
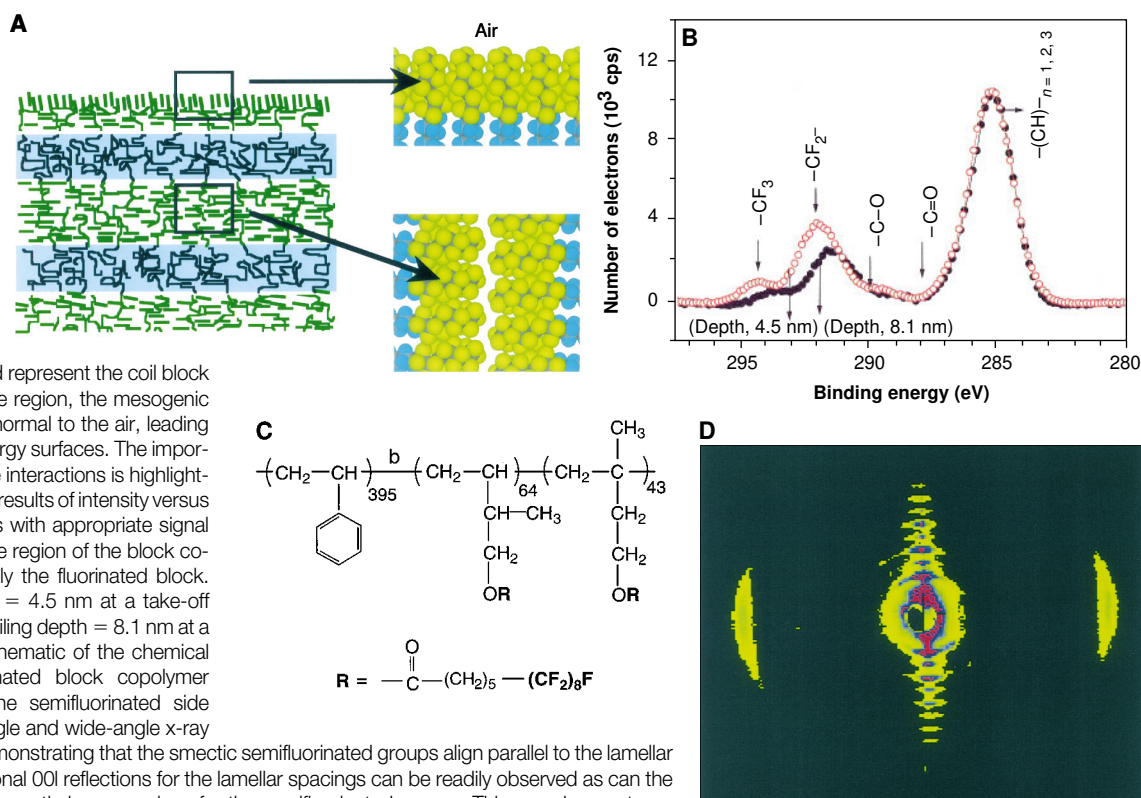
couple such ordering with the formation of finer scale structures by using more than one phase transition. Spontaneously organizing systems can be tailored by balancing such organizing forces as chemical incompatibility with others such as conformational entropy and liquid crystallinity. The resulting materials produce simultaneous organization on many length scales ranging from a few nanometers in the LC phase to
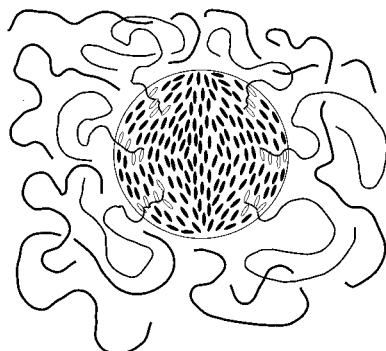
Fig. 5. Sketch of hierarchical structures in a mixture of a liquid crystalline AB diblock copolymer, an A flexible homopolymer, and a low molar mass LC solvent. The LC solvent mixes with the LC block and the flexible block blends with the matrix polymer to form the droplet interface. Such a structure can easily be used to create a polymer-dispersed LC display from several of the materials already described in this paper.

hundreds of nanometers in the phase-separated structures and even organization over micrometers in length in the surface-segregated materials. As early as 1977, Gallot and associates synthesized and studied lyotropic rod-coil block copolymers produced from polystyrene and a helical polypeptide block (24). Adams and Gronski produced LC block–coil block polymers by chemically modifying the diene block of a styrene-diene diblock copolymer so that cholesterol could be attached as a mesogenic side group (25). The LC phase was affected by confinement in the small, periodically spaced phase-separated domains of the polymer. Stupp and co-workers have synthesized a triblock copolymer of styrene-isoprene and a rodlike oligomer that aggregates to form unusual mushroom-shaped entities (26). In these materials, spontaneous noncentrosymmetric (polar) organization was reported and was presumably due to the nature of the supramolecular units of the copolymer preformed in the solution. Both microphase separation of the two coil blocks and the crystallization of the rod component play important roles in the selection of the unusual shape of the aggregate. This leads to the asymmetrical packing of the units, which form micrometer-sized plate-like objects exhibiting upper and lower surfaces that have hydrophobic and hydrophilic character, respectively.

Depending on the relative energetics, self-assembly can be driven through the LC transition or through the microphase transition. For example, rodlike homopolymers, because of their intrinsic chain stiffness, spontaneously form anisotropic LC phases in solution. The phase behavior of rodlike polymers can be controlled by either temperature or solvent concentration. The structures in rod-coil copolymers reflect the progression of a series of phase transitions from the dilute isotropic solution to the more concentrated nematic state, to the smectic microphase-separated state, to the final crystalline structure of the rod regions.

Some examples of novel rod-coil diblock structures that can be formed are illustrated by recent work on poly(hexylisocyanate-b-styrene) (PHIC-b-S) rod-coil block copolymers (27). Representative micrographs of two solid-state morphologies formed by rod-coils, one a smectic C (S_C) type and the other a smectic O (S_O) type structure, are shown in Fig. 3. In the PHIC–polystyrene (PS) system, as the solvent is evaporated, three phase transitions ensue: isotropic to nematic, nematic to smectic, and smectic to crystalline. By means of shearing the solution on a glass substrate when the system is in the nematic state, a globally oriented material can be formed. Because of the rather high molar mass of the PHIC rod com-

ponent, the smectic repeat is ~200 nm. Because of the long-range packing of the layers, correlation lengths easily reach the 10-μm scale. Electron diffraction confirms the helical packing of the PHIC block into a monoclinic unit cell with a c axis repeat of 1.56 nm. Interestingly, the very different packing requirements of the rod block compared with that of the coil block force rod-rod interdigitation as well as large rod tilt at the rod-coil interfaces in the S_C structure.

On the other hand, self-assembly of LC-coil block copolymers can be initiated by microphase separation, followed by the development of LC and crystalline ordering of more and more blocks. Mao et al. synthesized and examined diblock copolymers in which mesomorphic azobenzene groups were attached as side groups to an LC block formed from an isoprene backbone (28). In the lamellar block copolymers of this series, the axes of the mesogenic groups and the lamellar interfaces were parallel. Hexagonal cylinder morphologies made up of an LC block could also be produced (Fig. 3D).

There are distinctive molecular-scale features for the side chain and main chain LC block copolymer systems that lead to mesoscopic scale differences in their morphology. Typically, the mesogenic groups align parallel to the interface boundaries in side-group materials, but they align at a large angle to the interface in main-chain systems. This means that processing designed to manipulate the organization of the microstructure will also affect the global organization of the mesophase. By simple oscillatory shear, one may align the mesogenic groups in either the LC layers of a lamellar LC-coil block copolymer or the LC cylinders (or LC matrix depending on composition) in a cylinder block copolymer.

The ability to use the processing of the block copolymer microstructure as a means of manipulating the LC orientation is demonstrated by the example of LC-coil block copolymers in which chiral S_C (S_C^*) side groups are attached to the LC block (29). In such diblock copolymers, the helical S_C^* phase was oriented in a "bookshelf" arrangement that was produced by confining it to submicrometer domains oriented by simple shear alignment. In recent work (30), it was shown that no external alignment layers were needed, and the polymer film could be much thicker than conventional ferroelectric displays because it was processing of the block copolymer itself that was responsible for the LC orientation, not alignment by external surfaces. Moreover, the switchable films contained more mesomorphic material than comparable low molar mass films and led to large optical effects to create to the best of our knowledge the first successful example of bistable switching in a block copolymer film.

In the study of materials for the creation of low-energy surfaces, Wang et al. created a family of block copolymers into which semifluorinated groups were incorporated (31). Recent results demonstrate the possibilities to tailor such systems by balancing surface energy as well as LC behavior with microphase separation. These polymers typically have S_A or S_B phases, both of which orient on the basis of the arrangement of the internal interface of the lamellar or cylinder microstructure. In the semifluorinated LC blocks, remarkable degrees of spontaneous organization have been observed in lamellar systems. In these polymers, simply drying films from solution led to orientation of lamellae parallel to the substrate surface and within those layers; the fluorinated segments also lay parallel to the substrate. Contact angle measurements and Zisman analysis indicate that the surface is entirely populated by CF_3 groups rather than the CF_2 groups that might be assumed from the bulk organization of the film (Fig. 4). Recent near-edge x-ray absorption fine structure (NEXAFS) and x-ray photoelectron spectroscopy (XPS) results show that in the surface region, the semifluorinated groups project normal to the internal lamellar structure, which itself lies parallel to the surface. These latter results highlight the subtle effects that external surfaces and interfaces can have in such materials.

Challenges

The emerging challenges yet to be resolved may be expressed in two broad categories: extending hierarchically ordered structures to much larger length scales and sophisticated processing to form hierarchical structures with controlled ordering at different length scales. For the first category, we envision that, by topologically interconnecting self-assembled molecular architectures, new regimes of well-defined order at or above the technologically important wavelength-of-light scale may be attained in synthetic polymers. Such a premise immediately presents the following issues. (i) The size, shape, and decoration of the surface of a given domain with different kinds of chemical groups, as well as the surface area of each type of patch of such groups, are the various control parameters for each of the domains. The choice of the set of domains in the synthesis of MDP depends on the eventual utility of such structures and our level of understanding of self-assembly at mesoscopic length scales. (ii) Depending on the particular connectivity and the nature of the connectors, MDP polymers can be made, for example, as a linear array with flexible spacer groups, as a branched array, or even as two-dimensional sheetlike architectures. It is important to recognize that the specific interaction can lead to many topological states having only small differences in free energy, yet which present drastically different trajectories through the free energy landscape and can often easily frustrate the formation of the desired (not necessarily equilibrium) MDP structure.

For the second category of challenges, we envision that by integrating synthetic design with the design of specific processing pathways, the likelihood of attaining a targeted structure will be optimized. An example with an MDP structure is shown in Fig. 5, where a mixture of a LC block copolymer, flexible polymer matrix, and small-molecule LC solvent are the components. The issues that follow from such a scenario are the following: (i) Because multicomponent materials are involved, several physical phenomena such as phase separation, microphase separation, liquid crystallinity, crystallization, adsorption, vitrification, and various conformational transitions get coupled either synergistically or antagonistically during the self-assembly process. (ii) During the spontaneous formation of hierarchical structures, the local symmetry of an organizing domain may not be correlated with that in another domain. As a consequence, there are most likely defects in the structures. The free energy landscape of defects can be quite complicated, and extremely long times may be required for their annihilation. External fields, chemical potential gradients through solvent evaporation, temperature, and patterned substrates are ways to help guide the system toward the desired structures. Combined and pulsed external fields may also act synergistically instead of being simply additive.

The study of such materials and processes is already under way. Examples not cited above of the many attempts to provide structure by means of coupled interactions include the use of electric fields to process block copolymers and the creation of ordered gels and networks. Many new results are likely to occur in the next few years and will certainly lead to the ability to systematically tailor polymer structure and function to a much greater extent than is now possible. All of these challenges are interrelated, and advances need to be made in each of the areas outlined above.

REFERENCES AND NOTES

1. G. M. Whitesides, J. P. Mathias, C. T. Seto, *Science* **254**, 1312 (1991).
2. E. Reichmanis, C. K. Ober, S. MacDonald, T. Iwaynagi, T. Nishikubo, Eds., *Microelectronics Technology: Polymers in Advanced Imaging and Packaging* (ACS Symposium Series 614, American Chemical Society, Washington, DC, 1995).
3. P.-G. de Gennes, *Scaling Concepts in Polymer*

Physics (Cornell Univ. Press, Ithaca, NY, 1979); F. W. Wiegel, *Conformational Phase Transitions in a Macromolecule: Exactly Solvable Models in Phase Transitions and Critical Phenomena*, C. Domb and J. L. Lebowitz, Eds. (Academic Press, New York, 1983), vol. 7.

4. F. S. Bates and G. H. Fredrickson, *Annu. Rev. Phys. Chem.* **41**, 525 (1990).
5. For a discussion of several of the processes leading to self-organization, see special issue on the 1996 NATO Workshop on Tandem Molecular Interactions, in R. Zentel, G. Galli, C. K. Ober, Eds., *Macromol. Symp.* **117** (1997).
6. E. Dessipri, D. A. Tirrell, E. D. T. Atkins, *Macromolecules* **29**, 3545 (1996).
7. M. Muthukumar, *J. Chem. Phys.* **103**, 4723 (1995); *Comput. Mater. Sci.* **4**, 370 (1995).
8. For the specific example of diblock copolymers, the topological connectivity of various monomers in every chain appears as a density-density correlation at a distance *r* being proportional to $1/r$ so that $\alpha = 2$ (the Fourier transform of $1/r$ is $1/k^2$ in three dimensions). The long-range interaction can originate from such entropic correlations or electrostatic interactions (as in the case of surfactant and polyelectrolyte solutions) or chemical reactions (as in the case of simultaneous occurrence of macrophase separation and chemical reactions or hydrogen bonding).
9. The scheme requires consideration of shape and packing at the atomic and molecular level as well as at higher levels of scale leading to the three dimensional structure of the overall aggregate. Bringing the set of components together into the requisite array in a single process step (for example, by cooling the mixture) is extremely difficult, particularly when the basic units have conformational diversity under the conditions of the assembly process. Indeed, this situation is a critical issue, for if the system or parents of the system adopt wrong shapes and packings, then the desired structures may not even form.
10. A. H. Simmons, C. A. Michal, L. W. Jelinski, *Science* **271**, 84 (1996).
11. T. Gulik-Krzywicki, C. Fouquey, J.-M. Lehn, *Proc. Natl. Acad. Sci. U.S.A.* **90**, 163 (1993); M. Kotera, J.-M. Lehn, J.-P. Vigneron, *Tetrahedron* **51** (No. 7), 1953 (1995).
12. M. Müller, F. Kremer, R. Stadler, E. W. Fischer, U. Seidel, *Colloid Polym. Sci.* **273**, 38 (1995).
13. T. Kato, H. Kihara, U. Kumar, T. Uryu, J. M. J. Fréchet, *Angew. Chem. Int. Ed. Engl.* **33**, 1644 (1994); T. Kato, M. Nakano, T. Moteki, T. Uryu, S. Ujiie, *Macromolecules* **28**, 8875 (1995).
14. C. G. Bazuin, F. A. Brandys, T. M. Eve, M. Plante, *Macromol. Symp.* **84**, 183 (1994); C. G. Bazuin and A. Tork, *Macromolecules* **28**, 8877 (1995); R. Tal'roze, S. Kuptsov, T. Sycheva, V. Bezborodov, N. Plate, *ibid.*, p. 8689.
15. J. Ruokalainen *et al.*, *Macromolecules* **28**, 7779 (1995); J. Ruokalainen, G. ten Brinke, O. Ikkala, M. Torkkeli, R. Serimaa, *ibid.* **29**, 3409 (1996).
16. A. Pron, J. Lostra, J.-E. Österholm, P. J. Smith, *Polymer* **34**, 4235 (1993); T. Vikki *et al.*, *Macromolecules* **29**, 2945 (1996).
17. Peter R. Ashton *et al.*, *Angew. Int. Ed. Engl.* **36**, 735 (1997).
18. C. Gong and H. Gibson, *Macromolecules* **29**, 7029 (1996); G. Wenz, *Angew. Chem. Int. Ed. Engl.* **33**, 803 (1994).
19. C. K. Ober and G. Wegner, *Adv. Mater.* **9**, 17 (1997).
20. V. Percec and G. Johansson, *Macromol. Symp.* **95**, 173 (1995).
21. J. M. Park, B. B. Muhoberac, P. L. Dubin, J. Xia, *Macromolecules* **25**, 290 (1992).
22. E. L. Thomas, D. M. Anderson, C. J. Henkee, D. Hoffman, *Nature* **334**, 598 (1988).
23. J. M. Seddon, *Biochim. Biophys. Acta* **1031**, 1 (1990); T. Hashimoto, M. Takenaka, T. Izumitani, *J. Chem. Phys.* **97**, 697 (1992); J. Lauger, R. Lay, W. Gronski, *ibid.* **101**, 7181 (1994).
24. J.-P. Billot, A. Douy, B. Gallot, *Makromol. Chem.* **178**, 1641 (1977).
25. J. Adams and W. Gronski, *Makromol. Chem. Rapid Commun.* **10**, 553 (1989).
26. S. I. Stupp *et al.*, *Science* **276**, 384 (1997).
27. J. T. Chen, E. L. Thomas, C. K. Ober, G.-P. Mao, *ibid.* **273**, 343 (1996); J. T. Chen *et al.*, *Macromolecules* **28**, 1688 (1995).
28. G.-P. Mao *et al.*, *Macromolecules* **30**, 2556 (1997).
29. A. Omenat, R. A. M. Hikmet, J. Lub, P. Van der Sluis, *ibid.* **29**, 6730 (1996); W. Y. Zheng and P. T. Hammond, *Macromol. Rapid Commun.* **17**, 813 (1996).
30. M. Brehmer, R. Zentel, G. Mao, C. K. Ober, *Macromol. Symp.* **117**, 245 (1997).
31. J.-G. Wang, G.-P. Mao, C. K. Ober, E. J. Kramer, *Macromolecules* **30**, 1906 (1997).
32. We have benefited from interactions with many students and co-workers and would like to thank former members of our research groups. In particular, C.K.O. thanks G.-P. Mao and J.-G. Wang and E.L.T. thanks J. T. Chen. Funding from NSF (DMR-970527) (to M.M., C.K.O., and E.L.T.) and both NSF (DMR-9201845) and the Air Force Office of Sponsored Research (MURI PC 218975) (to C.K.O. and E.L.T.) is gratefully acknowledged. C.K.O. thanks the Office of Naval Research for support of the fluoropolymer work.

Fuzzy Nanoassemblies: Toward Layered Polymeric Multicomposites

Gero Decher

Multilayer films of organic compounds on solid surfaces have been studied for more than 60 years because they allow fabrication of multicomposite molecular assemblies of tailored architecture. However, both the Langmuir-Blodgett technique and chemisorption from solution can be used only with certain classes of molecules. An alternative approach—fabrication of multilayers by consecutive adsorption of polyanions and polycations—is far more general and has been extended to other materials such as proteins or colloids. Because polymers are typically flexible molecules, the resulting superlattice architectures are somewhat fuzzy structures, but the absence of crystallinity in these films is expected to be beneficial for many potential applications.

In the last two to three decades, materials science has developed into an interdisciplinary field that encompasses organic, polymeric, and even biological components in addition to the classic metals and inorganics. Although carbon-based molecules offer an enormous structural diversity and tunability in terms of potential properties or processability, they also typically suffer from a lack of stability when exposed to heat, oxidizing agents, electromagnetic radiation, or (as in the case of complex biomolecules) dehydration. Multicomposites make it possible to combine two or more desirable properties, as in the classic reinforced plastics, or to provide additional stability for otherwise highly labile functional biomolecules or biomolecular assemblies. Even higher device functionality will arise from a combination of physical and chemical processes (such as electron or energy transfer) and chemical transformations found in nature (such as photochemical energy conversion). Such devices require control of molecular orientation and organization on the nanoscale, as their function strongly depends on the local chemical environment. It is therefore highly desirable to develop methods for the controlled assembly of multicomponent nano-

structures, although it is also clear that structures as complex as those found in the biological world, such as the flagellar motor, cannot yet be fabricated.

It is, however, possible to consecutively deposit single molecular layers onto planar solid supports and to form multilayers in which nanoscale arrangements of organic molecules can be controlled at least in one dimension (along the layer normal). This approach also fulfills another prerequisite for functional macroscopic devices: a fixed relation between nanoscopic order and macroscopic orientation. To fully exploit an assembled structure, it is necessary to know the location or orientation (or both) of every molecule, not only with respect to each other (as in ordered or phase-separated bulk systems at the nanometer scale, such as liquid crystals, copolymers, or zeolites), but also with respect to a macroscopic coordinate. Only materials that have such structural hierarchy (*1*) allow molecular properties to be fully exploited in macroscopic devices, as, for example, in organic waveguides for second-order nonlinear optics or in biosensors.

In simple multilayer systems, this demand is reduced to the sequence of layers and to the orientation of molecules with respect to the layer normal. For about 60 years, the molecularly controlled fabrica-

Université Louis Pasteur and CNRS, Institut Charles Sadron, 6, rue Boussingault, F-67083 Strasbourg Cedex, France. E-mail: decher@ics-crm.u-strasbg.fr